Force Measurements on Locusts During Visually-Evoked Collision Avoidance Maneuvers

Rajeev Kumar[1], Raymond Chan[2], Sergey Shkarayev[3,*] and Fabrizio Gabbiani[4,*]

[1]Assistant Research Professor, University of Arizona, Tucson, AZ, Department of Aerospace and Mechanical Engineering, rajeevk@email.arizona.edu, Member AIAA

[2]Research Associate, Baylor College of Medicine, Houston, TX, Department of Neuroscience, rchan@cns.bcm.edu

[3]Professor, University of Arizona, Tucson, AZ, Department of Aerospace and Mechanical Engineering, svs@email.arizona.edu, Senior Member AIAA

[4]Associate Professor, Baylor College of Medicine, Houston, TX, Department of Neuroscience, gabbiani@bcm.edu

[*]These two authors contributed equally to this work

Received 21 May 2012, Accepted 31 August 2012

ABSTRACT

The collision avoidance behavior of the locust, Schistocerca americana, in response to simulated approaching objects, also called looming stimuli, was investigated in a low speed wind tunnel. The animals were mounted using a sting on a sensitive six-component microbalance custom-designed for the experiments. Forces and moments were measured as a function of time during the simulated approach and interpreted in the context of collision avoidance behaviors. The stimuli presented from the side effectively evoked robust and discernible collision avoidance responses. Locusts attempted to avoid collision by either flying over or under the looming object, or alternatively by steering around it. These efforts appeared in the form of changes in aerodynamic forces and moments as a function of time. It was also observed that the locusts increased the wing flapping frequency in response to the stimulus.

NOMENCLATURE

m_b	reference body mass of locust, *g*
l_b	reference body length of locust, *mm*
W	reference body weight of locust, *N*
U	tunnel velocity, *m/s*
L_r	relative lift, vertical component of aerodynamic force normalized by W
T_r	relative thrust-drag, horizontal component of aerodynamic force normalized by W
S_r	relative side force, sideway component of aerodynamic force normalized by W
l_r	relative rolling moment, rolling moment normalized by W and l_b
m_r	relative pitching moment, pitching moment normalized by W and l_b
n_r	relative yawing moment, yawing moment normalized by W and l_b
f	flapping frequency, *Hz*
e	hysteresis, *%*
θ	angle subtended by the stimulus on the animal's retina, *deg*
σ	standard deviation
R	correlation coefficient
t_{vP}	Student *t*-estimator with v degrees of freedom and a P^{th} percentile confidence level

1. INTRODUCTION

The inability of fixed wing Micro Air Vehicles (MAVs) to fly at low speeds and their poor maneuverability have inspired the development of flapping wing MAVs, also known as ornithopters, mimicking birds and insects. However, both fixed wing as well as flapping wing MAVs have been found to be prone to collisions in their most desirable application of providing low-altitude surveillance in urban and in challenging military settings. Insects, especially locusts, have attracted great attention because of their ability to fly in swarms in which millions of individuals may be spaced as little as 30 cm apart and rarely collide [1]. Their ability to maneuver quickly and correctly in such dense swarms is of great interest for engineering as it points to robust visuo-motor control mechanisms [2]. Furthermore, locusts possess in their brains collision sensitive neurons that are involved in the generation of collision avoidance responses. All these factors have contributed to the extensive use of insects, and especially locusts, in collision avoidance research. Wing movements are central to these studies as they generate the aerodynamic forces and moments required in these avoidance maneuvers. Evidence of strong linkages between these wing movements and neural activity has inspired research across disciplines from neurobiology to robotics and aerodynamics.

The aerodynamics of insect flight, as we know it today, is dominated by unsteady mechanisms involving three-dimensional flow structures [3, 4]. However earlier theories of bird and insect flight were based on conventional aerodynamics [5-8] (reviewed in [9]) supported by experimental data [10, 11]. Jensen [11] first measured average forces on flying locusts and determined wing postures by cinematographic analysis. He then tested the detached wings in the same postures in a wind tunnel and found that steady state aerodynamics could be applied to locust flight. Cloupeau et al [12] later conducted wind tunnel tests on intact desert locusts to confirm Jensen's results [11]. These authors found that the lift variations observed during a beat cycle were far greater than those observed on detached wings. Wilkin [13] confirmed Cloupeau's results and also calculated wing inertial components.

From a broader perspective, various researchers have experimented with a variety of species and models to better understand insect flight. Dudley and Ellington [14] for instance used bumblebees to measure aerodynamic forces and power requirements in forward flight. Sane [15] employed a dynamically scaled mechanical model of the fruit fly to study wing kinematics and unsteady aerodynamic forces. Combes and Daniel [16] investigated the contributions of aerodynamic and inertial-elastic forces to wing deformation in the hawk moth *Manduca sexta*. Hawk moth wings compliance was also studied by Mountcastle and Daniel [17] and their structural dynamic properties by Sims et al [18].

Recently, a number of wind tunnel experiments have been conducted on the tethered desert locust, *Schistocerca gregaria* [19 – 22]. Taylor and Thomas [21] generated extensive force measurement data to study dynamic flight stability while Taylor and Zbikowski [22] used instantaneous force-moment measurements to parameterize the non-linear rigid body equations of motion in a time-periodic model.

The neural basis of visually guided collision avoidance during flight in locusts is amenable to detailed scrutiny because of their experimentally accessible nervous system. Elucidation of these neural mechanisms and their aerodynamic implementation could be valuable for MAV development. Locusts possess on each side of their brain an identified visual neuron, the Lobula Giant Movement Detector (LGMD), which responds selectively to approaching threats and faithfully conveys that information to motor centers generating escape responses through a second neuron called the Descending Contralateral Movement Detector (DCMD). The varying activity of the LGMD-DCMD was linked to various stages of jump escape behaviors [23]. Computer generated two-dimensional simulations of approaching objects (looming stimuli) presented to either eyes from the side of the animal are sufficient to evoke vigorous responses in the LGMD-DCMD [24, 25]. The intensity of this response decreases as the trajectory of the simulated colliding object is offset from the midpoint of the eye, indicating that the LGMD-DCMD neurons are tuned to objects approaching on a direct collision course [26].

In early behavioral experiments on collision avoidance behaviors in flight, Robertson and Reye [27] used objects approaching from the front to study wing and body kinematics in the tethered migratory locust, *Locusta migratoria*. They found that objects on a direct collision course altered the wing beat pattern and induced changes in body posture consistent with movements away from the approaching object. In a follow-up study, Robertson and Johnson [28] confirmed these results with limited force measurements. Gray et al [29] recorded the activities of right and left DCMDs in migratory locusts in response to visually simulated targets approaching from the front along different trajectories. They

found that locusts are more sensitive to trajectory changes in the horizontal plane than in the vertical plane. Their results also suggested that the DCMD could be better suited to predator evasion than avoiding obstacles in the animal's flight trajectory.

Santer et al [30] recorded the steering movements and wing beat patterns of tethered migratory locusts in response to looming stimuli presented from the side, a situation that mimics attack from a predator. They observed a rapid stereotyped behavior, known as 'glide', in which the locust briefly ceases to flap its wings for about 200 ms and thereafter flaps its wings with increased frequency. Rind et al [31] tested more than 150 migratory locusts to study the effect of arousal in this collision avoidance behavior. Their results suggest an important role for the neuromodulator octopamine in maintaining the sensitivity of the DCMD to approaching stimuli in flight.

Recently, we investigated the collision avoidance behaviors of the locust, *Schistocerca americana*, flying loosely tethered in a wind tunnel to looming stimuli presented on the side of the animal [32]. We found a variety of collision avoidance behaviors distinct from the 'glide' behavior previously reported in tethered animals. In the present work, we extend this study by measuring the time-varying aerodynamic forces and moments generated by tethered locusts to the same stimuli. Our main objective was to describe typical models of collision avoidance maneuvers, and to study the effect of variation of the looming stimulus trajectory on the collision avoidance behavior of the animals.

2. EXPERIMENTAL SETUP

The experiments were conducted in a low speed wind tunnel. A six-component microbalance, a sting for mounting locusts on the balance, high-speed video cameras (Photron FASTCAM SA3), a LabVIEW based data acquisition system and the locust, *Schistocerca americana* (closely related to the desert locust, *Schistocerca gregaria*) were parts of the experimental setup explained in following sections.

2.1. Wind Tunnel

The low-speed wind tunnel (Fig. 1) is an open circuit wind tunnel with a 91.44 × 60.96 × 60.96 cm closed test section (length × width × height; 3 *ft* × 2 *ft* × 2 *ft*). The contraction ratio is 6.25:1 and can produce wind speed between 0.25 and 5 m/s with a reasonably low turbulence level (<0.5%).

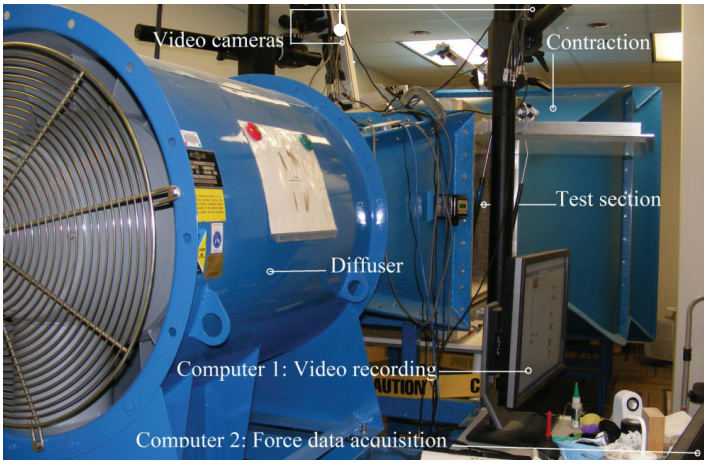

Figure 1. Low speed wind tunnel at Baylor College of Medicine.

2.2. Six-component Microbalance and Sting

Low Reynolds number experiments typically involve very small forces and often require experiment-specific balance designs. The highly unconventional mode by which insects generate aerodynamic forces also needs to be taken into consideration. A sensitive, custom-built 6-component microbalance has been used in this study (Fig. 2). It consists of a platform that rests through pins on three gram-force load cells for measuring normal force components and three additional load cells that are connected to the platform through wires along the horizontal directions to measure the thrust and the side force components. These load cells (Transducer Techniques, Model GSO-30) are capable of measuring

forces as small as 2 mg. The balance has provisions to mount artificial flapping wings as well as insects. The insect mounting mechanism consisted of a sting made out of a carbon tube with a steel nail cemented on top and a threaded rod on the other end. The bottom end with the threaded rod slides snugly into a hole drilled on a small Plexiglas block that is attached to the balance (Fig. 2). A small micro-magnet was glued at the top of the nail. The microbalance was installed under the test section floor by placing it leveled atop a table (Fig. 2). It was positioned such that the sting passed through the projection of the tunnel centerline on the test section floor. A white Plexiglas sheet then placed on the floor of the wind tunnel covered the balance such that only the sting protruded out of a hole as shown in Fig. 2.

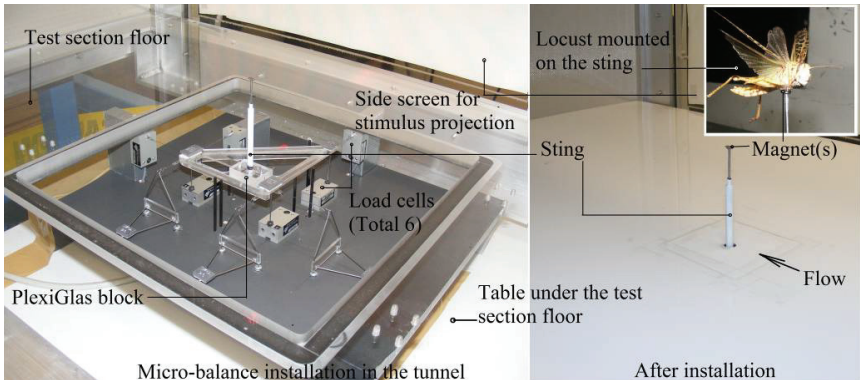

Figure 2. Microbalance installed in the tunnel and insect mounted on the sting (inset).

2.3. Locusts and Tethering

The adult locusts were selected from the laboratory colony. The locusts were tethered to the sting using a pair of strong micro magnets (size: 6 *mm* × 3 *mm* × 1 *mm*; weight 0.1 g). One of these magnets was cemented on the flat surface of the nail fixed to the top end of the sting as shown in Fig. 3. The second magnet was cemented to the locust's sternal sclerites forming the plastron of the pterothorax using cyanoacrylate adhesive.

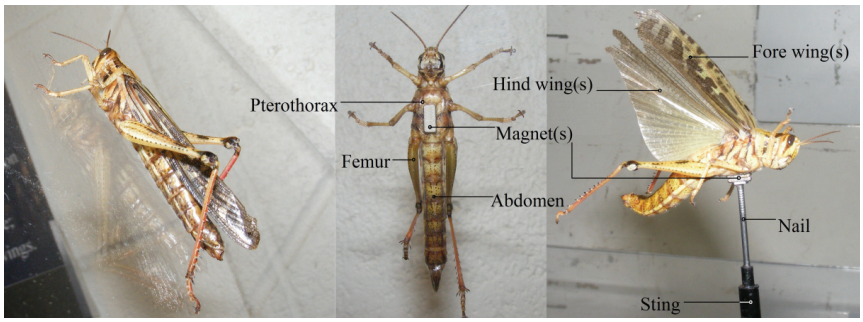

Figure 3. Locust, *Schistocerca americana*, and tethering.

The animals were initially selected based on the condition of their wings and appendages. They were then tested for their readiness and stability of flight in a large room. The good flyers were then mounted on a sting placed in front of a tabletop fan to further test their flight capabilities under restrained conditions. The insects were weighed before each experiment using a sensitive scale (Mettler Toledo PB153-5; resolution: 1 mg). Generally younger and lighter locusts are known to be good fliers, therefore young adults with body mass ranging between 1.0 g – 1.75 g were employed with the specifications presented in Table 1.

Table 1: Specifications for the locusts tested

Locust	Total runs (good ones)	Reference body mass, *g*	Reference body length, *mm*	Center of mass location*, *mm*
1	10 (9)	1.066	39.0	4.8
2	5 (5)	1.282	40.0	4.9
3	6 (3)	1.731	45.0	5.0
4	10 (8)/ **16 (16)**†	1.410	40.0	5.0
5	6 (6)	1.505	41.0	5.0
6	8 (7)	1.265	40.0	5.0
7	10 (8)	1.210	39.5	4.8
8	**16 (16)**†	1.335	40.0	5.0

*Approximate distance to center of mass above the pterothorax,
†Runs conducted in phase 2 to see the effect of changing the target trajectory

2.4. Definition of Forces and Moments

The right-handed coordinate system used and the definition of aerodynamic forces and rotations is shown in Fig. 4. Since the tests were conducted at zero body angles (*angle of attack* and *yaw angle*), the body coordinate system (x_b, y_b, z_b) coincides with the tunnel coordinate system (x, y, z). Moments were resolved at the center of mass of each locust. We estimated the location of the center of mass based on the results of Taylor and Thomas [21]. These authors determined the center of mass using a model aircraft propeller balancer and approximately located it at the midpoint of a 2 mm wide slice starting from the place where the hind leg of the insect meets the pterothorax. Accordingly, the approximate location of the center of mass was about 5 mm from the magnet attached to the animal's thorax. The center of mass locations for individual locusts were added to the length of the sting to resolve moments at that location. Figure 4 also displays a schematic of the looming stimulus projected from the left sidewall of the test section.

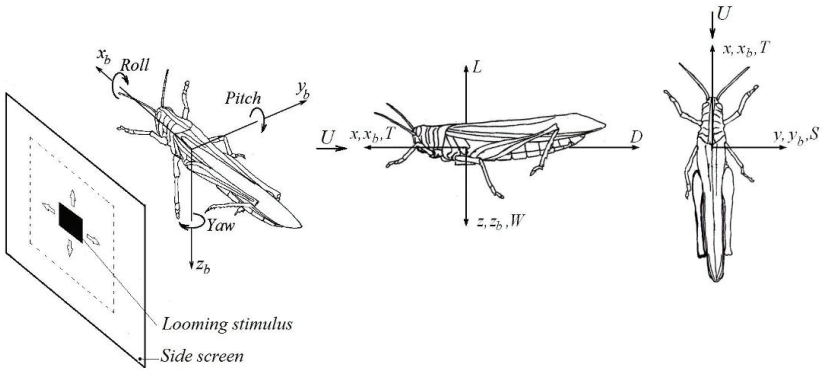

Figure 4. Coordinate systems and definition of forces and rotations. (x, y, z) is the coordinate system fixed to the tunnel and (x_b, y_b, z_b) is the coordinate system fixed to the locust. The looming stimulus is projected on the left side screen. (L: lift, D: drag, U: air speed, W: weight, T: thrust and S: side force)

2.5. Data Acquisition System

The data acquisition system consists of a National Instruments SCXI 1000 Chassis housing a SCXI-1600 USB 16-bit digitizer module, an 8-channel strain gauge input module SCXI-1520 with add-on terminal 1314, and a computer with LabVIEW software for data acquisition and analysis (PC2 in Fig. 5).

2.6. Looming Stimulus Projection and Triggering System

A computer is used to generate the looming stimuli, trigger the video cameras and acquire video data (PC1 in Fig. 5). This computer generates looming stimuli using MATLAB code and the psychophysics toolbox (www.psychtoolbox.org). The schematic in Fig. 5 explains the experimental setup, looming

stimulus projection and the triggering process. Briefly, video recordings and the second computer (PC2) are triggered from PC1 using TTL (Transistor-Transistor Logic) pulses.

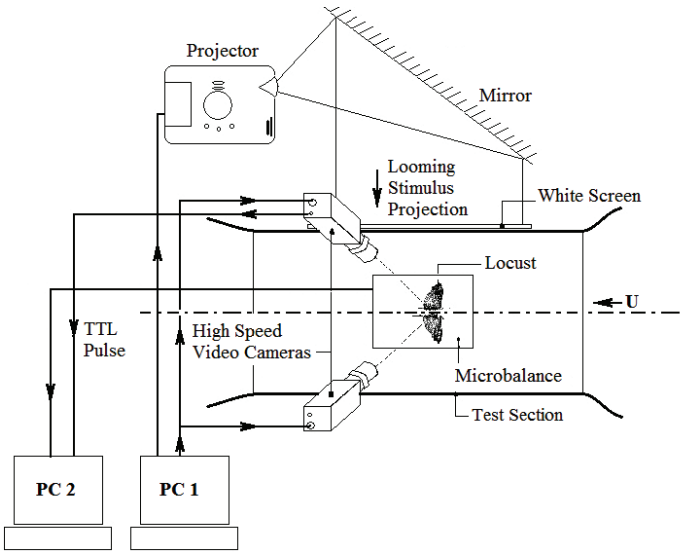

Figure 5. Schematic showing the top view of the experimental setup, looming stimulus video projection and triggering.

3. BALANCE CALIBRATION AND ACCURACY

The 6-component balance was calibrated by successively loading the load cells one by one and recording the strain output in *mV/V*. Note that each load cell is effectively a full Wheatstone bridge. In order to account for the coupling among the load cells, the output was recorded from all the elements at each load. Load cells were loaded incrementally from the no-load condition to about 10 g and then unloaded in the same steps all the way back to the no-load condition. Loading in the thrust direction was done by applying stepwise horizontal loads at the top of the micro-magnet fixed at the top of the sting. Calibration results revealed that the coupling among the load cells was minimal resulting in negligibly small off-diagonal elements in the 6×6 coefficient matrix.

Typical calibration results for the six load cells corresponding to diagonal elements of the coefficient matrix are described here. The best-fit lines and correlation coefficient, R were computed using MS Excel, while the standard deviation, $\boldsymbol{\sigma}$, and hysteresis, $\boldsymbol{e}$, were computed as the percentage of the full output scale as described in Figliola and Beasley [33]. The correlation coefficient for the six load cells was in the range $0.9998 < R < 1.0$, the hysteresis percentage in the range $0.242\% < e < 0.535\%$ and the standard deviation in the range $0.0177 \text{ g} < \sigma < 0.0193 \text{ g}$.

Temperature-induced changes in resistance in the Wheatstone bridge circuit can result in an output signal indistinguishable from that produced by the loads being measured. The signal conditioner and the rest of the data acquisition circuits can also be affected by temperature and become an additional source of 'instability'. The term 'instability' in strain gauging, also known as 'zero drift', denotes random deviations in the signal when the loading conditions are stationary. In our setup, the zero drift over a period of 2 hours was about 1%. This is acceptable considering the fact that our typical experimental recording time was about 30 seconds.

The accuracy of the balance was estimated by applying known loads and moments and measuring them. The load and moments measurements were repeated 4-6 times and a regression analysis was carried out on the results to estimate their linearity and their standard deviation. A 95% confidence interval was estimated by using the *Student-t distribution* table (*p. 122*, ref. 33). A typical result for the thrust element measurement is given by $\tilde{y} = 0.9993\, x - 0.00051 \pm 2.201 \times 0.01636$, where x represents the known load and $\tilde{y}$ the measurement. The format is $\tilde{y} = mx + c \pm t_{vP} \times \sigma$, where m is the slope and c the intercept of the regression line, t_{vP} is the t value for the P^{th} (95^{th}) percentile value of the Student-t distribution with v degrees of freedom (equal to 11 for thrust data).

4. EXPERIMENTS

The experiments spanning over a couple of weeks were conducted at a tunnel velocity of 2.0 m/s, body angles of attack and yaw equal to 0°, and with the tunnel temperature maintained at approximately 30 °C. Locusts are known to settle into optimum aerodynamic performance at a body angle of attack of about 7° [21]. The objective in this study, however, was to effectively capture the collision avoidance responses rather than to record the optimum aerodynamic performance of the insects. Therefore a body angle of attack equal to 0° was chosen which warranted minimum adjustments to the experimental setup. For video recordings, the test section was illuminated with red light to minimize interference with the looming stimulus and since locust photoreceptors are insensitive to it.

Normally, the average of 5000 samples obtained from the balance with the insect mounted on the sting and no wind would have been used as offset nulling values. However, while taking the null reading some of the locusts would grab the sting with their front legs. Afterwards they would not flap their wings, even with the wind turned on. Therefore an alternative way of taking the null reading was adopted, with no insect and no wind. The locust was mounted on the sting only with the wind turned on after taking the null readings. The null voltages obtained in each of the element of the microbalance were adjusted for the weight of the locust as:

$$V_{null\ adjusted}\left(mV/V\right) = V_{null}\left(mV/V\right) + m_b(g) \times sensitivity\ \ (mV/V/g) \tag{1}$$

where V_{null} is the null voltage in any element of the balance, m_b the mass of the locust, and the sensitivity was determined from the calibration procedure described above.

Forces and moments were measured without locust (i.e. with only sting and nail) multiple times and the averaged values were subtracted as tare from the actual measurements with the insect mounted on the sting. Data were acquired at a sampling rate of 1000 samples/s for 15 seconds. High-speed videos were recorded for about 8.2 seconds at a rate of 500 frames/s.

Experiments were carried out in two phases. In the first phase, seven locusts were tested with a fixed looming stimulus trajectory (designated as looming trajectory 1, see following section) and 5 to 10 runs were conducted on each. In the second phase, four different looming trajectories were tested, including looming trajectory 1 that was used in phase 1. One locust (locust 4) could be kept from the first phase and two new locusts (locust 8 and 9) were selected in addition to locust 4. Details of the four different stimulus trajectories follow.

4.1. Looming Stimulus Trajectories

In this section, we describe the visual stimuli in general terms; a quantitative description is provided in Appendix 1. All stimuli mimicked the approach of a solid black square on a direct collision course with the animal by projection onto a two-dimensional screen. Such stimuli are called looming stimuli. Phase one of the tests was carried out with a looming stimulus that expanded symmetrically around the center of the screen. Initially, the stimulus subtended less than 2º at the center of the screen and increased up to a maximal angular size of 86º over a total approach time of 5.75 s. Since the animal's eye was located 20 cm below the center of the screen, the stimulus effectively mimicked a black square approaching the animal's eye from above on a direct collision course and at a constant speed. This stimulus is designated as looming stimulus 1. Looming stimulus 1 and three additional variants employed in phase 2 of the tests are shown in Fig. 6(a). In looming stimulus 2, the expansion is centered at the same height as the locust eye, thus simulating a direct horizontal collision course trajectory with the animal at constant speed. As illustrated in Fig. 6(b), the angle subtended by the object at the eye is in this case uniquely determined by the ratio between the object's half size, l, and the approach speed, $|v|$. For all stimuli, $l/|v|$ was equal to 40 ms. In looming trajectory 3, the stimulus starts at the top of the screen, grows and expands to full screen while descending. Effectively, it mimics an object approaching the animal from the top. In looming stimulus 4, it starts at the bottom of the screen as shown in Fig. 6, and eventually grows to full screen while ascending, effectively representing a case where an object would approach the locust from below. In these last two stimuli the approach speed was not constant: the object effectively decelerated as it was approaching the animal, thus mimicking a predator swooping down or up on the animal. The angles subtended on the animal's retina by the four stimuli as a function of time are presented in Fig.6(c).

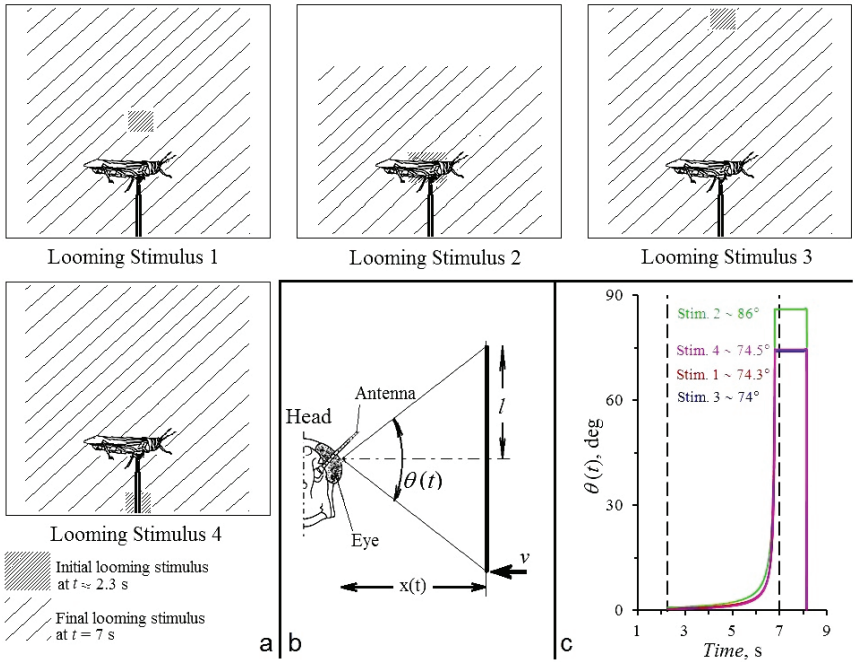

Figure 6. (a) Different looming stimuli based on their projection on the screen and (b) angle subtended by the stimulus on the retina of the left locust eye during a direct horizontal approach (looming stimulus 2). Note that $\tan[\theta(t)/2] = l/vt$, where l is the object's half-size and v is its approach velocity. By convention, $v<0$ for an approaching object, t is measured relative to collision time and < 0 before collision. (c) Angle subtended on the retina by the different looming stimuli as a function of time since trial onset.

4.2. Looming Stimulus Projection

The looming stimulus was delivered with the help of a projector and a mirror on a white rear projection screen mounted on the left external side of the test section window (Fig. 4). A typical example is shown in Fig. 7 where three snapshots of the projection sequence for looming stimulus 1 are presented. The screen remains blank during the first 2.25 seconds of the projection during which the locust flies normally. At t = 2.25 seconds, a small black square appears at the center of the screen. The initial location of this point differs for different looming trajectories as discussed in the previous subsection. The size of the square increases gradually and smoothly until t = 7 s when it has expanded to cover the full screen (except for stimulus 2).

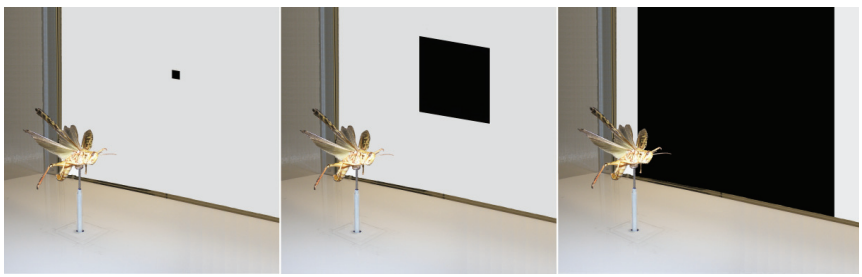

Figure 7. Three snapshots of a typical looming stimulus projection sequence (looming trajectory 1 shown).

4.3. Post-Processing of Microbalance Data

The raw analog data were converted into six time series of forces and moments using the calibration coefficient matrix. Because of the high sensitivity of the load cells, the raw data contained noise and frequency components unrelated to the animal's movements. To eliminate them, the raw data were

therefore filtered using a 10th order low pass Butterworth filter in MATLAB. The filter's cutoff frequency was set to three times the locust wing flapping frequency (f). The flapping frequency, typically close to 20 Hz, was calculated by spectral analysis of the data in MATLAB. It was also seen that spurious frequencies of about 28 – 30 Hz were lying between the first and second harmonics of the flapping frequency. These spurious frequencies, were found to be caused by the mechanical vibrations of the balance and were particularly significant in thrust and side force measuring load cells. They affected the periodic nature of the forces and moments concerned. A 10th order band stop Butterworth filter was used to eliminate these frequencies. The order of the filter was set by very low values of the selected pass-band ripples, R_p = 0.7 dB and the stop-band attenuation, Rs = 40 dB. The quality of the signals considerably improved as is evident from Fig. 8, where a typical time series of the lift and net horizontal force (for locust 3, run 1) are displayed over an interval of 0.2 s before and after filtering along with the fore-wing tip trajectories for the period. A discernible rhythmic pattern of the forces related to the wing beat cycle emerges in the filtered traces that cannot be discerned in the noisy raw data. It can also be seen from the figure that the peaks in lift and thrust occur during the downstroke (Fig. 8b and 8c). In our measurements, the time course of forces and moments changes substantially on the time scale of the locust wing beat cycle (50 ms), whereas the looming stimulus expands on a much longer time scale, on the order of seconds. Because we were interested in relating changes in forces and moments to the time course of the looming stimulus, we carried out further averaging of the data. As illustrated in Fig. 9, a running average of the thrust during a single trial over a temporal window ranging between 0.5 and 1 s captures well the overall aerodynamic trend of the data. Thus, in Figs. 10-18, we present single trial data sub-sampled at regular time intervals Δt = 1.0 s and averaged over these intervals. Additionally, we present the mean response across all trials, obtained by taking the running average of single trials over a temporal window of 1 s and then averaging the resulting traces across all trials.

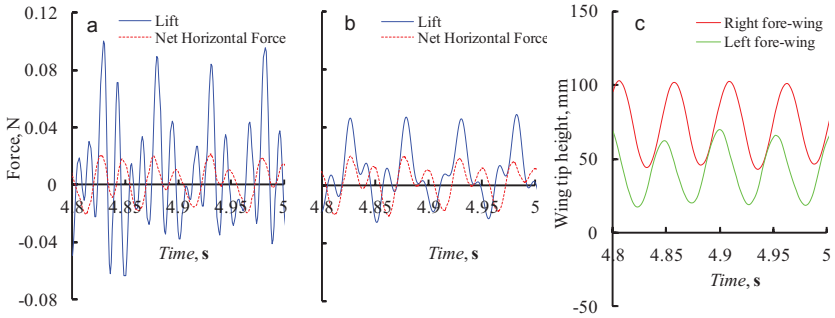

Figure 8. Effect of filtering on the acquired signal, Locust 3, run 1. (a) Raw traces of forces. (b) Traces after filtering. (c) Trajectories of the fore-wing-tips.

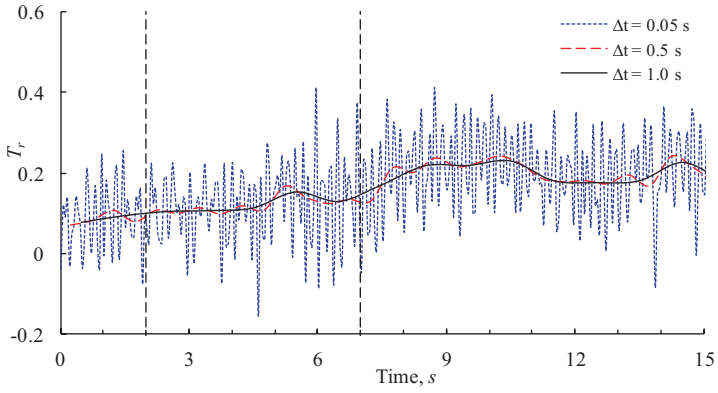

Figure 9. Capturing the overall trend of the aerodynamic behavior by averaging. Dashed vertical lines indicate the stimulus presentation epoch.

In this study, we analyzed changes in forces and moments because they are indicative of changes in behavior. Any constant offset in the forces and the moments either due to minor experimental setup misalignments or due to idiosyncrasies associated with the insect's behavior were disregarded. Trials where the variations in forces and moments were apparently random and contained long inactive periods on the part of the locust were discarded (see Table 1).

5. RESULTS AND DISCUSSION

The experiments were conducted in two phases. In the first phase, the collision avoidance behavior of seven locusts was investigated with looming stimulus 1. The main objective was to find out the general behavioral trends of locusts in the tight tether configuration required to measure forces and moments. In the second phase, we tested whether the behavioral patterns change in parallel with the looming trajectory.

Each trial consisted of three main segments spread over 15 seconds of recorded data. The first segment, from 0 – 2.25 s, is the pre-stimulus flight segment. The second segment, between 2.25 s and 7 s, starts with the looming stimulus appearing on the screen. In this segment the locust flies with the object looming towards it and expanding to cover the entire screen at $t = 7$ s. The third segment covers the post-stimulus epoch from 7 s to 15 s. Results were analyzed by averaging across trials and at the level of single trials by sub-sampling and averaging over the sub-sampled time windows (see sect. 4.3). Single trial traces of forces and moments were often useful to explain variations in the behavior observed in the average across trials.

5.1. Collision Avoidance Responses to Looming Stimulus 1

Seven locusts were tested in this phase 1 with body masses between 1 g – 1.8 g. Results suggested that mass generally did not have much influence on the type of avoidance reaction exhibited by the animals, except that the locust with largest mass (locust 3) exhibited a tendency to move sideways into the stimulus and roll towards it just before projected collision. All of them otherwise generally attempted to fly higher, faster and away from the approaching stimulus, as indicated by the rising lift, thrust and side force levels. Additionally, they generally tended to roll and yaw away from the stimulus with positive pitching moment. In the following subsections, the avoidance responses of three locusts spanning the body mass range are presented (light, intermediate and heavy).

5.1.1. General Behavior of a Light Locust

Ten runs were carried out on locust 1 which was the lightest with mass, $m_b = 1.066$ g. Figs. 10a and 10b respectively depict the forces and moments generated during the avoidance responses normalized by body weight (i.e., relative forces and moments, see the nomenclature). Two dashed vertical lines at $t = 2.25$ s and $t = 7$ s indicate the emergence and the complete expansion of the looming stimulus on the screen, respectively. The locust responded after 2.25 s by increasing its lift and thrust seen as a hump in their plots roughly between $t \approx 2.3$ s and t ≈ 6 s (Fig. 10a). The side force showed a mild increase indicating some efforts by the locust to move sideways, away from stimulus. Correspondingly, a similar hump appears in the pitching moment and rolling moment plots (Fig. 10b). This indicates that the insect seemingly tried to roll away from the approaching object by tilting the wing nearer to the stimulus up with a nose-up pitching attitude. The locust's reaction in the early part of the looming epoch therefore seems to be to fly higher, faster and steer away from the object by generating positive roll. This is consistent with observations by Robertson and Reye [27] who found that upon early detection of a rapidly moving object approaching from the front in their field of view, locusts attempt either to fly over it or to steer away from the object.

Interestingly just before the looming stimulus reaches its maximal size on the screen (at $t = 7$ s), there is a sudden dip in lift, thrust and pitching moment marking the end of the corresponding humps at $t \approx 6.5$ s. Again there is very little variation in side force and yawing moment. Since at that time the looming object is very large, this response suggests that the locust attempted to suddenly lose lift and slow down, in other words tried to suddenly lose altitude. As far as moment generation is concerned, it tried during this maneuver to generate nose-down pitching moment and roll towards the looming object as a mild decrease in roll indicates. Robertson and Reye [27] and later Santer et al [30] documented a similar response by *Locusta migratoria*, in which upon late detection of the looming object the locust straightened the wings up, stopped flapping for a short duration of about 0.3 s which would result in a quick loss of height and speed. They termed this maneuver a 'glide' and interpreted it as a last chance

evasive response to avoid collision or being caught by an aerial predator [27, 30]. This maneuver is evoked only when other steering maneuvers have either failed or it is too late to initiate them. Analogous short sequences of gliding flight lasting roughly 0.3 s were recorded under natural conditions by Baker and Cooter [34]. After this sudden drop in lift, thrust, pitching moment and rolling moment, there is a subsequent sharp increase in lift, thrust, side force and pitching moment around t = 7 s. Furthermore, a mild rise in rolling and yawing moments accompanies it. These changes are consistent with a post stimulus avoidance response, in which the locust having perceived a persistent threat, seemingly attempted to escape it by flying higher, faster and away from the stimulus and, in doing so, generated mild positive rolling and yawing moment with nose-up pitching moment. Afterwards, at about t = 9 s, approximately 2 s after the looming stimulus stopped expanding, the locust returned to its normal flight pattern, with a level of forces and moments comparable to those of the preceding free flight.

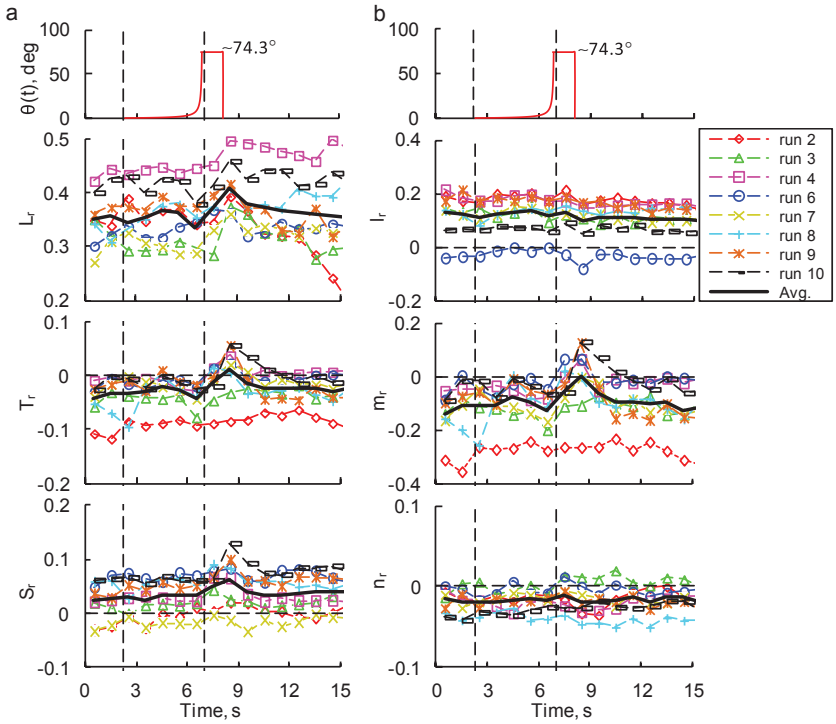

Figure 10. (a) Averaged force responses of locust 1 (m_b = 1.066 g) to looming stimulus 1. (Top) Time course of the angular size of the approaching object subtended at the animal's eye (see Appendix 1). (b) Averaged moment responses.

5.1.2. General Behavior of an Intermediately Heavy Locust

This locust (locust 4) with mass, m_b = 1.41 g was about 40% heavier than locust 1 and lies in the middle of the weight range tested. Ten runs were conducted on it, with two of them rejected. At the onset of the looming stimulus, the reaction of the locust is a little different from that of locust 1. This animal reduced its lift considerably with a mild decrease in thrust up until $t \approx 5.5$ s. Side force remained more or less unchanged (Fig. 11a). Rolling moment during this time period remained unchanged indicating no rolling tendencies. It had a nose-up pitching tendency and almost no yawing tendency (Fig. 11b). Therefore the insect's behavior during the initial part of the looming stimulus can be summed up as an attempt to fly under the looming object without rolling and with a mild nose-up pitching moment. This is one of the strategies also observed by Robertson and Reye, as locusts seem to detect a frontally approaching object [27]. At $t \approx 5.5$ s the locust changed behavior. At that time, the looming object is sizable on the screen, increasing its threatening appearance. In the previous case of locust 1 we observed a response seemingly similar to a 'glide' at this point. However, in this case no glide is noticeable. This is possibly because the locust has already been trying to fly under the looming object.

As the looming stimulus reaches its maximal size, the locust attempted another escape maneuver. In this case it sharply increased lift, thrust and side force at t = 7 s (Fig. 11a). Correspondingly, it mildly rolls away from the stimulus, with a strong nose-up pitching tendency and practically no yawing (Fig. 11b). This response can be interpreted as an attempt to fly fast over the looming object and away from it as the rise in rolling moment indicates. This is again one of the strategies observed during frontal collision avoidance by Robertson and Reye [27]. This surge in forces and sharp moment change starts subsiding at $t \approx 8$ s with normal flight conditions thereafter.

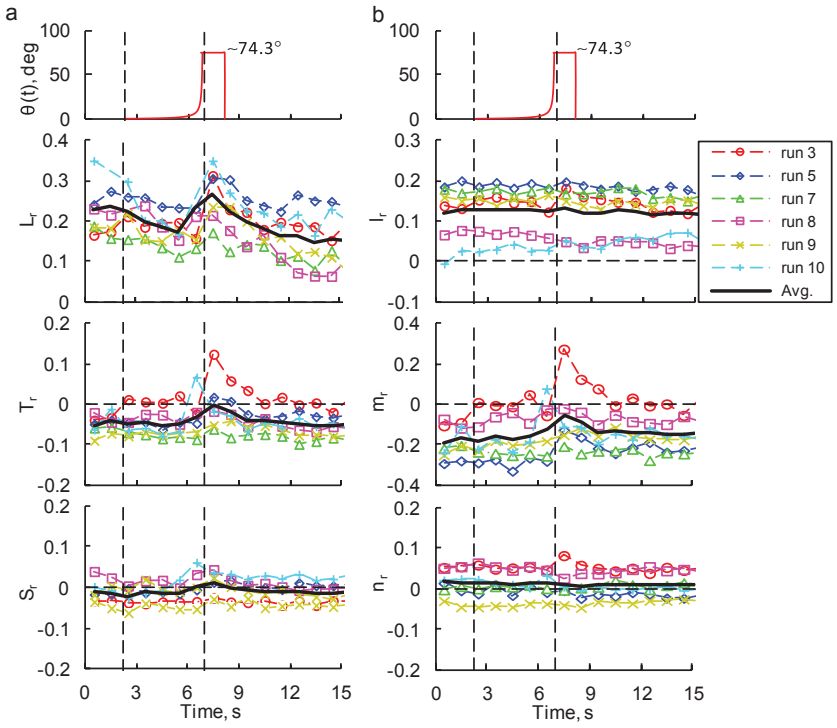

Figure 11. (a) Averaged force responses of locust 4 (m_b = 1.41 g) to looming stimulus 1. (Top) Time course of the angular size of the approaching object subtended at the animal's eye (see Appendix 1). (b) Averaged moment responses.

5.1.3. General Behavior of a Heavy Locust

Locust 3 with m_b = 1.731 g, almost 75% heavier than locust 1, was the heaviest among the locusts tested. Collision avoidance responses based on four good runs out of six in total are presented in Fig. 12. Unlike the previous two, this locust mostly generated a net positive thrust, which means it was able to overcome the aerodynamic drag. Its average relative lift was also much higher, although like the other two locusts it did not generate enough lift to support its weight. This is not surprising since tethered locusts were found to generate weight-balancing lift only at optimal speeds of about 3.5 m/s and a body angle of about 7∞ [9, 10]. Tests in the current study were conducted at 2 m/s with a 0∞ body angles. Robertson and Reye [27] also observed in their experiments that tethered locusts never generated lift large enough to support their weight.

Similar to the first locust, this one started responding at $t \approx 3.5$ s by increasing its lift and thrust but in contrast to locust 1 it moved towards the looming object as is evident from a mild decrease in the side force in Fig 12a. Its pitching moment and rolling moment increased after initial decrease whereas the yawing moments remained almost unchanged suggesting that the locust tried to fly over the looming object with a nose-up pitching attitude and a hint of rolling towards it initially, followed by a roll away from it. In earlier experiments, locusts resorted to this type of response when they detected the threat early enough [27]. This maneuver continued until $t \approx 5.5$ s when a sharp drop in lift, thrust and a sharp increase in side force occurred (Fig 12a). A drop in rolling and pitching moment also

occurred for a brief period of time, between 5.5 s – 6.0 s, resembling to a 'glide' maneuver. At this time the looming stimulus appears large and threatening. Lift and thrust rise sharply but the side force drops indicating it tended to move toward the stimulus. Sharp variations in the moments much like those seen in lighter locusts follow this maneuver with the exception that this locust tended to roll towards the stimulus as indicated by a decline in rolling moment. So the heavy locusts like the lighter ones attempted to fly faster and above the object but unlike lighter ones they showed a tendency to move and roll towards the approaching stimulus just before the projected collision.

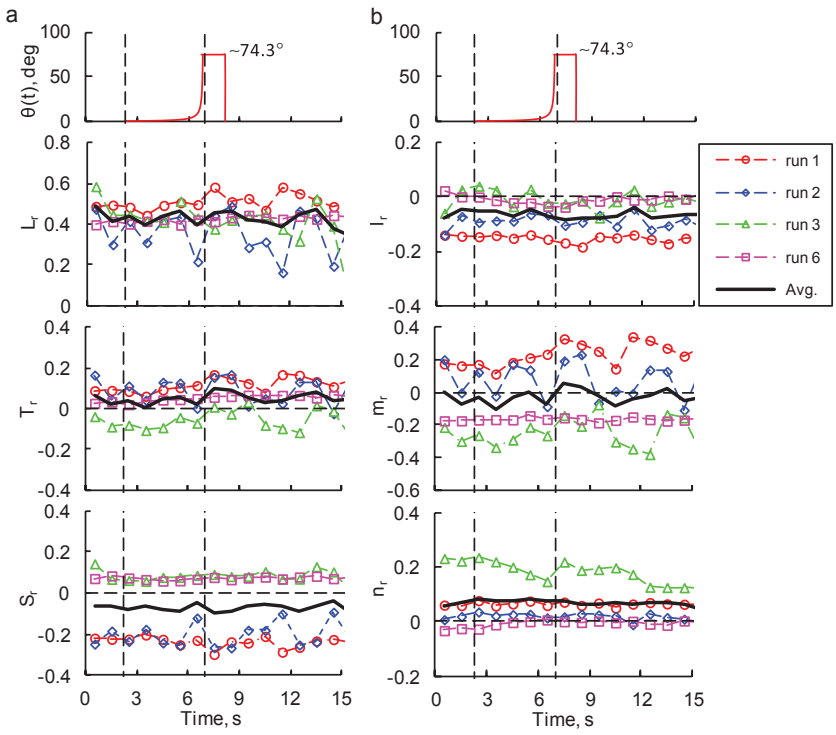

Figure 12. (a) Averaged force responses of locust 3 (m_b = 1.731 g) to looming stimulus 1. (Top) Time course of the angular size of the approaching object subtended at the animal's eye (see Appendix 1). (b) Averaged moment responses.

5.2. Effect of Variation of Looming Stimulus on Locust Response

Three locusts (locust 4, 8 and 9) were tested with four different looming stimuli (see Fig. 6) to assess the effect of simulated trajectory on the avoidance behavior. Typical results for locust 8 (m_b = 1.335 g) are presented.

5.2.1. Response to Looming Stimulus 1

Results based on three good runs out of a total of four runs with trajectory 1 are presented in Fig. 13. As seen in Fig. 13a, this locust was able to generate fairly large aerodynamic forces, especially thrust in excess of drag. A steady increase in lift and thrust suggests that the locust detected the looming stimulus early and attempted to fly over it. The usual dip in lift related to the 'glide' maneuver and the subsequent jump in force levels thereafter is replaced by a steady rise in forces well past the end of the looming stimulus. The side force remained more or less steady. The rolling moment remained almost constant, and the pitching moment showed a nose-up tendency throughout, while yaw increased a little (Fig. 13b). Thus, this locust seemingly chooses to avoid the object by flying over it while steering away from it [27].

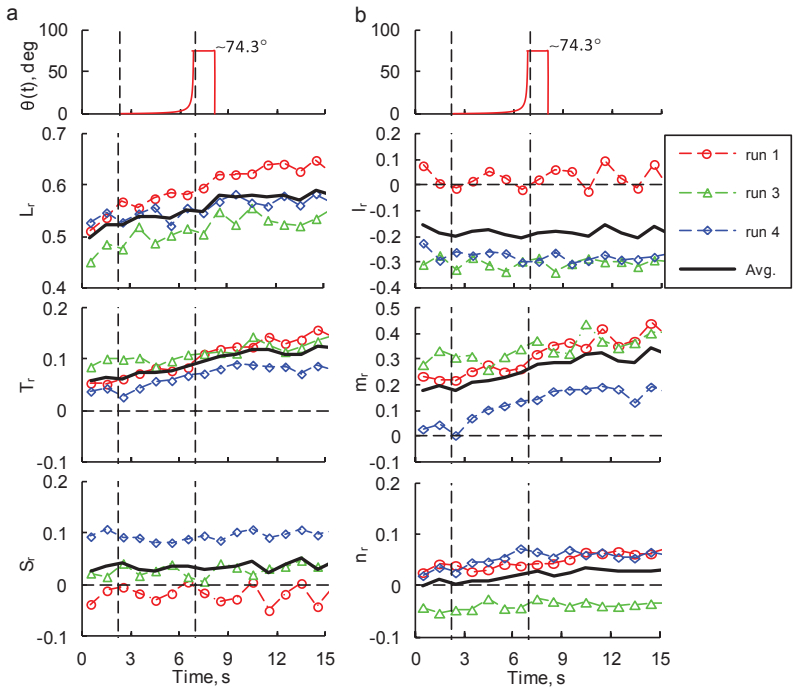

Figure 13. (a) Averaged force responses of locust 8 (m_b = 1.335 g) to looming stimulus 1. (Top) Time course of the angular size of the approaching object subtended at the animal's eye (see Appendix 1). (b) Averaged moment responses.

5.2.2. Response to Looming Stimulus 2

This looming stimulus starts expanding at the same height as the locust, but does not eventually fill the full screen. It simulates a target approaching the locust on a direct horizontal collision course in contrast to looming stimulus 1, which approaches from above. The immediate reaction shown by the locust includes raising lift, thrust and pitching moment to fly over the approaching target. There is practically no change in side force indicating it did not try to move away from target sideways (Fig 14a). Here too there is no sign of a 'glide' maneuver just before the end of looming at t = 7 s. Instead, the forces rise faster around that time. Furthermore, the rolling and yawing moments show a slow rise indicating that the locust attempts to fly over the object with a mild rolling and yawing away tendency (Fig. 14b). Levels of forces and moments tend to stay at somewhat higher levels after the end of looming, once the apparent threat is gone.

5.2.3. Response to Looming Stimulus 3

Looming stimulus 3 mimics an object approaching from the top of the screen on a descending trajectory, as may occur during an attack from a predator approaching from high above in a swooping maneuver. Eventually this stimulus expands to cover the full screen. Four runs were carried out using this stimulus on locust 8 and responses have been categorized into two types.

5.2.3.1. Response Type 1

The first type of response is shown in Fig. 15. The locust initially maintained the lift, thrust and side forces almost constant up to $t \approx 6.5$ s. They then increased slightly near t = 7 s when the stimulus was in its final expansion stage. Immediately afterwards the locust drastically reduced lift and thrust in an extended 'glide'-like maneuver. The locust seems to have tried to fly under and away from the looming stimulus as can be seen from the sharp decrease in lift and thrust accompanied by a gradual increase in side force in Fig. 15a. Correspondingly, there is a sharp increase in rolling moment and a small increase in yawing moment during this extended 'glide'-like maneuver (Fig. 15b). The decreasing lift (hence altitude), lowering thrust (hence speed) and sharply decreasing pitching moment suggest that the locust tried to glide down with nose-down attitude. It also tried to roll and yaw away from the approaching object coming from top. Usually locusts resume flapping after the 'glide' maneuver [27, 30], bringing about a sharp increase in lift, thrust and moments but this locust resorted to an extended glide down and apparently did not resume

flapping. This, although rare, yet not surprising because Santer et al [30] in their study conducted in *Locusta migratoria,* observed that while most of the locusts resumed flight after a glide with increased wing beat frequency, some locusts folded their wings at the end of a glide rather than resuming flight.

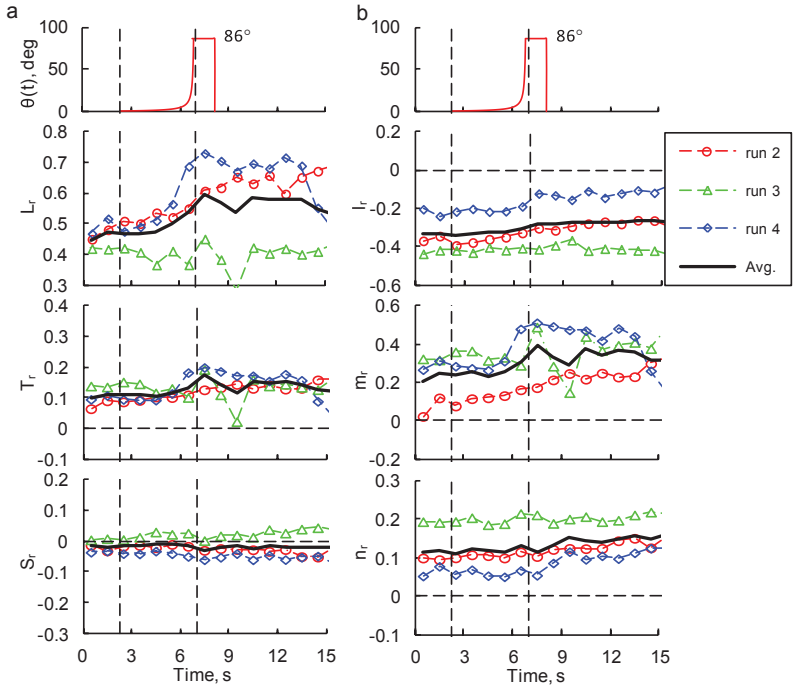

Figure 14. (a) Averaged force responses of locust 8 (m_b = 1.335 g) to looming stimulus 2. (Top) Time course of the angular size of the approaching object subtended at the animal's eye (see Appendix 1). (b) Averaged moment responses.

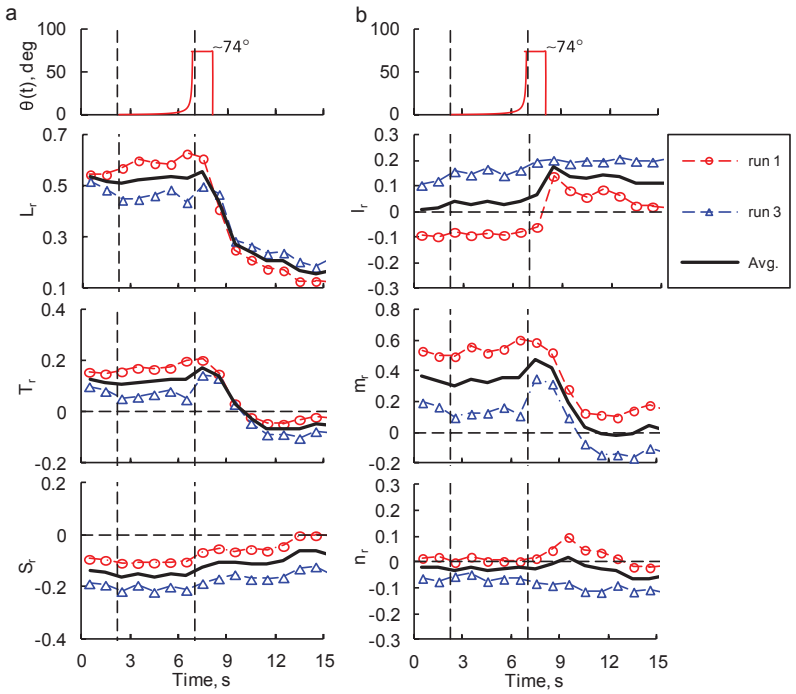

Figure 15. (a) Averaged force responses (type 1) of locust 8 (m_b = 1.335 g) to looming stimulus 3. (Top) Time course of the angular size of the approaching object subtended at the animal's eye (see Appendix 1). (b) Averaged moment responses.

5.2.3.2. Response Type 2

The locust behaved in a distinctly different manner in two of the four runs conducted with looming stimulus 3, mimicking an approach from high above in a swooping maneuver. It responded in the early part of the looming by raising the lift, thrust and pitching moment, eventually reaching a sort of plateau. Towards the end of the looming stimulus, the locust resorted to a 'glide' maneuver followed by a weaker than usual increase in forces, presumably in an escape attempt (Fig. 16a). The difference here is that the 'glide' maneuver which usually occurred just before t = 7 s occurred a little after 7 s. The rolling moment decreased during the 'glide' and increased after that. This means that the locust initially rolled towards the stimulus and attempted to roll away from it afterwards, as can be seen in Fig. 16b. The pitching moment decreased mildly during the 'glide' and increased thereafter. This means that the locust tried to lose altitude and speed while rolling towards the object with a nose down pitching attitude for a moment when the stimulus would have hit it and a maneuver quickly followed by an attempt to fly faster upwards with a nose-up attitude and rolling away from the approaching object.

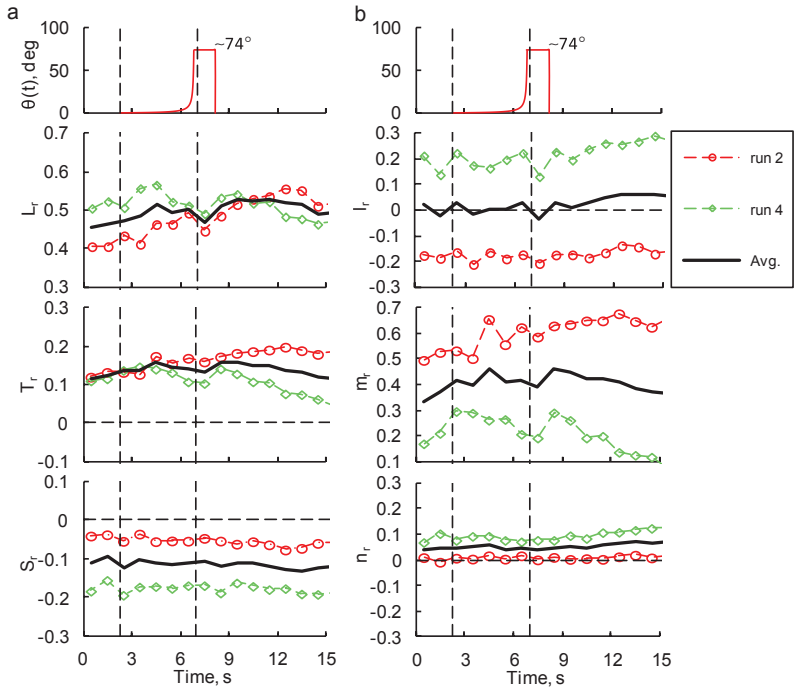

Figure 16. (a) Averaged force responses (type 2) of locust 8 (m_b = 1.335 g) to looming stimulus 3. (Top) Time course of the angular size of the approaching object subtended at the animal's eye (see Appendix 1). (b) Averaged moment responses.

5.2.4. Response to Looming Stimulus 4

In this case, the presented stimulus started at the bottom of the screen and expanded fully, effectively simulating an object approaching the insect from below in a swooping maneuver. The locust started responding as soon as the stimulus appeared on the screen at $t \approx 2.25$ s by steadily raising its lift, thrust and pitching moment but keeping the side force constant as seen in Fig. 17a. This suggests an attempt to fly over the looming object with a nose-up pitching attitude as reported by Robertson and Reye for frontal approaches [27]. The rolling and yawing moment remained more or less constant except around t = 7 s, where there is a hint of increase suggesting that the locust tried to steer away from the looming object (Fig. 17 b). The yawing moment showed a mild tendency to rise, indicating that the locust attempted to yaw away from the object.

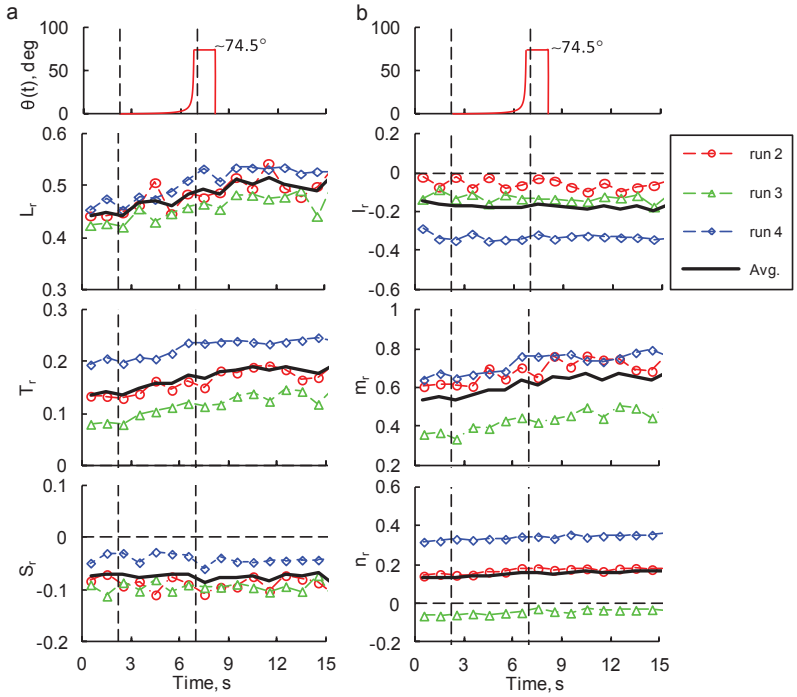

Figure 17. (a) Averaged force responses of locust 8 (m_b = 1.335 g) to looming stimulus 4. (Top) Time course of the angular size of the approaching object subtended at the animal's eye (see Appendix 1). (b) Averaged moment responses.

5.3. Typical Collision Avoidance Behavior Models

In the past sections, the collision avoidance behavior of eight locusts with body masses between 1 and 1.8 g were studied over 70 runs conducted with four different looming stimuli. Each stimulus started at t = 2.25 s and expanded to its maximal size on the screen at t = 7 s (Fig. 5). The results suggest that the responses of the locusts can be broadly grouped into five typical behavior models, as explained in the following sections, with one example case for each model.

5.3.1. Behavior Model 1

This is the most common behavior exhibited by the locusts. They started responding to the looming stimulus almost immediately and seemingly attempted to avoid collision by flying over the object with a simultaneous roll away maneuver and a nose-up pitching tendency. This is evident from the increase in lift, thrust, rolling moment and pitching moment. Locusts usually exhibit this type of immediate reaction when they detect the object early [27]. This tendency continues up until $t \approx 6$ s. Around this time the looming stimulus expands increasingly fast on the screen and may cause the locust to perceive an imminent threat that triggers a maneuver resembling a 'glide'. A sudden drop in lift and thrust and a concurrent sudden rise or drop in angular moments characterizes this maneuver. The 'glide' may be attempted by locusts as a last ditch effort to avoid imminent collision with a predator [27, 30]. During the short period of the 'glide', lasting about 0.3 s, they would lose altitude quickly thus helping avoid the predator. Baker and Cooter have indeed documented glides in natural conditions [34]. This maneuver is followed by a sharp rise in lift, thrust, side force and, most of the time, rolling moment, as well as a sharp rise in pitching moment as a further attempt by the locust to presumably escape the stimulus. This model can be summed up as an attempt to *initially fly over the object, then glide and escape the scene by flying faster upwards while rolling and yawing away from object*. The responses of locust 1 in Fig. 10 are an example of this typical behavioral model.

5.3.2. Behavior Model 2

This behavior model is characterized by a highly variable flight trajectory between $t \approx 3$ s to $t \approx 6.5$ s followed by a clear attempt to lose lift and fly fast under the stimulus. In the example illustrated in Fig.

18, the locust started responding to the looming stimulus at about $t \approx 3$ s by seemingly attempting to fly over it, which resulted in increased lift, thrust, side force and pitching moment (Fig. 18a). The rolling and yawing moments remained constant during this period suggesting no efforts to roll or yaw away from the path (Fig. 18b). It decreased and increased lift between $t \approx 4.5$ s and $t \approx 6.5$ s. Finally at about $t \approx 6.5$ s it seemingly attempted an extended 'glide'-like maneuver where lift, thrust and pitching moment dropped sharply with almost no change in side force. During this extended 'glide' period between $t \approx 6.5$ s to $t = 7.5$ s, the rolling moment and yawing moment showed a slow rise (Fig. 18b). This indicates that the locust attempted to lose altitude, and more so than in a usual 'glide', with a nose-down pitching attitude. At this time the stimulus is expanding maximally on the screen presumably greatly increasing the perceived threat. This extended glide is followed by an increase in lift, thrust, side force, as well as pitching moment. The yawing moment remained constant and there is a hint of rise in the rolling moment. At that point, the locust seemingly tried a further escape maneuver, maintaining lower altitude by keeping the lift lower than that observed before the extended glide. Interestingly, locust 4 ($m_b = 1.41$ g) exhibited this behavior model in response to looming stimulus 3, which simulates an object approaching from above. So this behavior model can be summed up as *an initial erratic attempt to fly over the target followed by an extended 'glide'-like maneuver that would result in considerable loss of altitude and thereafter an accelerated low escape flight with a mild rolling away tendency.*

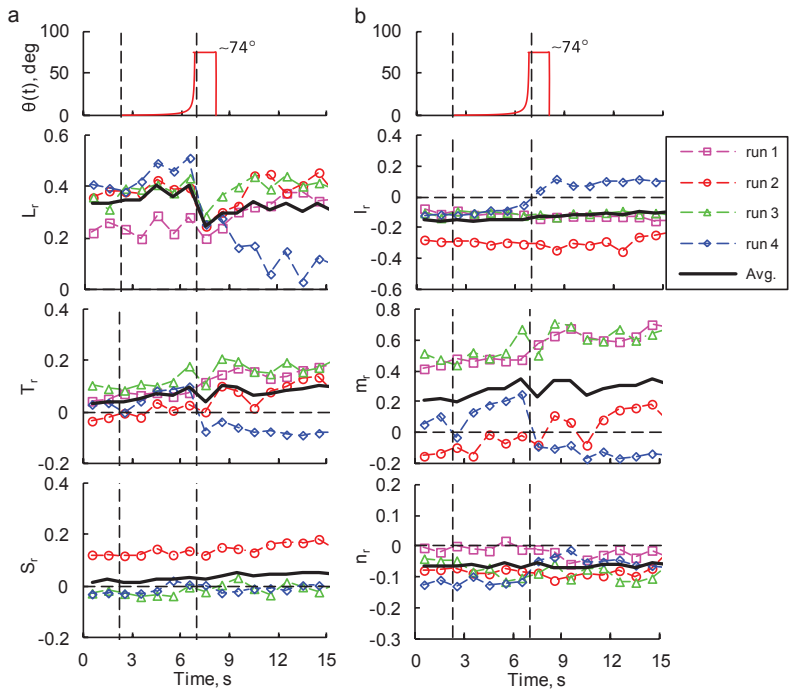

Figure 18. (a) Averaged force responses of locust 4 ($m_b = 1.41$ g) to looming stimulus 3. (Top) Time course of the angular size of the approaching object subtended at the animal's eye (see Appendix 1). (b) Averaged moment responses.

5.3.3. Behavior Model 3

This model is characterized by an early detection of the looming stimulus and thereafter an effort to fly over it with a steady increase in lift and thrust, with a nose-up pitching attitude. The side force, the rolling and the yawing moments remain almost constant indicating the locust attempted to 'fly over' indicated by a steady increase in speed and altitude. This model is represented by the behavior of locust 8 ($m_b = 1.335$ g) in response to looming stimulus 1 (Figs. 13a and 13b) as well as to looming stimulus 4 (Figs. 17a and 17b). The behavior model can be summed up as an attempt to *fly fast over the object without much rolling and yawing*.

5.3.4. Behavior Model 4

This type of behavior resulted from the responses of locusts to looming stimulus 2 as illustrated in Fig. 14 by locust 8. Here the locust sees the object looming at same height and therefore in direct collision course with it. It started responding at about $t \approx 4$ s by sharply increasing lift, thrust an pitching moment, with a mild increase in the rolling and yawing moment, indicating an attempt to fly upwards steeply with a rolling away tendency. This effort continued until little beyond 7 s when the looming stimulus ended. There were then indications of a slow down but soon the level of forces generated by the locust picked up again and tended to remain high thereafter. This flying model can be summed up as an attempt to *fly over the object as fast and as steeply as possible while rolling and yawing away.*

5.3.5. Behavior Model 5

This behavior model is illustrated by locust 8 responding to looming stimulus 3 (shown in Fig. 15), which simulates an approach from above. It is characterized by normal flight until about the sixth second of the trial. At this point the stimulus grows increasingly fast on the screen. The locust for a brief while tried to accelerate upwards and away from the object as a brief rise in lift, thrust, side force and pitching moment indicates (Fig. 15a). Immediately after that, the locust appears to attempt an extended 'glide'-like dive to avoid the threat that seems to come from above. This translates in a steep decrease in lift, thrust and pitching moment. The side force increased, indicating that the locust attempted to fly away from the object. The sharp increase in rolling moment suggest an attempt to roll away from the stimulus while flying downwards. This behavior model can be summed up as an attempt to *fly normally and when the object is about to hit, to simply drop down fast with a roll away*.

5.4. Wing-Beat Cycle Analysis

In addition to the time averaged force and moment analysis presented above, Five randomly selected trials of locust 1 tested with looming stimulus 1 were analyzed by taking twenty cycles from the free-flight segment and the post-collision segment. Parameters like the maximum, the minimum and the amplitude of the forces and moments in each cycle were found and averaged over the twenty cycles. We observed an increase in the lift, thrust and side force peaks accompanied by a corresponding change in moment peaks due to more vigorous down-strokes in response to the looming stimulus (the peaks of lift and thrust occur during the down stroke [11, 12]). Spectral analysis of the instantaneous data from these two flight segments showed up to 10% increase in the flapping frequency. Robertson and Johnson [28] in their experiments on *Locusta migratoria* recorded about 20% increase in the wing-beat frequency due to more vigorous down-strokes by the locust during collision avoidance.

This increase in flapping frequency in response to the looming stimulus generally raised the levels of maxima, minima and average values of instantaneous lift, thrust and side forces. An increase of about 8% - 20% in mean lift was observed which indicates a tendency to fly higher. Thrust-drag increased from a generally negative value in phase 1 to a positive value in phase 3, which meant that the locust started generating net thrust presumably in an effort to escape. Similarly, about 10% - 90% increase in side force indicates a strong tendency to move away from the stimulus. In line with theses tendencies there was up to 43% increase in rolling moment and up to 57% increase in yawing moment indicating a strong tendency to roll and yaw away from the approaching stimulus. The pitching moment showed a strong nose up tendency. These moment characteristics are consistent with the fact that locusts generally attempted to escape away from the looming stimulus.

The generation of extra forces and moments was possible due to the extra power generated through the increased flapping frequency (~10%). The average wing tip velocity, V_T is given by $b\,\Phi f$, where b is the wing span, Φ is the flapping amplitude and f the flapping frequency. Any increase in the flapping frequency would increase the reference velocity that would in turn result in an increase in the aerodynamic forces and moments generated.

CONCLUSIONS

We studied the mechanisms underlying the generation of collision avoidance behaviors in response to looming stimuli with simultaneous force measurements and high-speed video recording on the locust *Schistocerca americana*. The main objective of this study was to develop an experimental setup to effectively evoke collision avoidance responses in tethered locusts, and to measure those responses in the form of aerodynamic forces and moments as a function of time. This allowed us to define prototypical models of collision avoidance maneuvers, and to study the effect of variation of the

looming stimulus trajectory on the avoidance behavior of the locusts. The study was also aimed at understanding the kinematics of the flapping wings in response to the looming stimulus. A very sensitive custom built six-component microbalance was used to measure aerodynamic forces and moments. Inertial forces have not been accounted for in this study.

The looming stimulus was presented from the side on a white screen positioned on the sidewall of the tunnel. Based on our results, we conclude that this setup effectively evoked collision avoidance responses in the set of locusts tested. The avoidance responses measured in the form of aerodynamic forces and moments as function of time were sufficiently significant and robust to be clearly evident and interpretable as attempted escape maneuvers.

Locusts responded to the stimulus in the initial stages of looming by attempting to either (a) flying over it, (b) fly under it, or (c) steer around it. These behaviors appeared in the form of increases or decreases in lift, thrust and side forces. The steering away tendencies caused rolling and yawing moments. The pitching moment increases or decreases seemed to be associated with efforts to fly upwards or downwards, respectively.

In the later stages of looming, just before the stimulus ended, the insects tended to respond with a behavior that seemed to represent a last ditch effort to avoid the collision and named 'glide' by various researchers [27, 30, 34]. This maneuver was characterized by a sudden drop in lift and thrust for a brief period during which the locust would lose height quickly in order to avoid the simulated object. This was usually followed by a sharp rise in lift and thrust, as well as side forces in some cases. Depending on whether locust tried to fly over straight or steer around the stimulus, there were sharp variations in moments.

The behavior patterns described previously generalized to all the seven locusts having body mass in the range of 1 g - 1.8 g tested with stimulus 1. The type of avoidance response exhibited by the locusts was generally insensitive to mass although the heaviest locust tested exhibited a mild tendency to move sideways and roll towards the stimulus just before the collision.

The trajectories of the looming stimulus were varied in order to see its effect on the locusts' collision avoidance behaviors. We observed that whenever the looming stimulus was presented from below, locusts generally tried to fly upwards without resorting to 'glide' maneuvers. When the stimulus was presented from the top towards the locust, it resorted to a long 'glide'-like maneuver triggered around the end of the stimulus.

Locusts increased noticeably their wing flapping in response to the looming stimulus. In the process, there generally was an increase in peak lift and thrust and a decrease in minimum lift and thrust during the wing beats. This resulted in an increase in average lift and thrust. Interestingly a 5% – 10% concurrent increase in the wing-beat frequency was recorded which is most likely one of the reasons for the increase in lift and thrust.

APPENDIX 1

The looming stimuli simulated a black square of half-size l, approaching the rear projection screen at a constant horizontal velocity, v, on a trajectory perpendicular to it, as illustrated in Fig. A1. If $Y(t)$ denotes the horizontal distance from the animal's eye to the object, then $Y(t) = vt$, where t denotes time relative to collision. Hence, $t = 0$ at collision and, by convention, $t < 0$ before collision. Consequently, for an approaching object $v < 0$. The looming stimuli were generated by central projection from a point c, located at a distance $d_{as} = 318$ mm from the screen and aligned with the center of the approaching square. In the case of looming stimulus 1, this point coincided with the center of the screen, located at a vertical distance $z_0 = 200$ mm above the animal eye. In the case of stimulus 2 the object was approaching on a horizontal trajectory centered on the eye and the center of projection coincided with the animal's eye ($z_0 = 0$). In the case of looming stimuli 3 and 4 the center of projection moved vertically down or up according to the equation $c(t) = \alpha t + z_0$, with $\alpha = \pm 50$ mm/s and $z_0 = 200$ mm. For stimulus 2, the angle subtended by the object on the animal's retina is fully determined by the ratio $l/|v|$ of the square's half size and its approach speed as may be seen from the trigonometric relation $\tan \theta/2 = l/vt$. From similar triangles, we see that the half-height of the object on the screen is given by $z_{cu}(t) = ld_{as}/vt$. In the general case of a moving center of projection, $c(t)$, the upper and lower edges of the object on the screen are given by $z_u(t) = z_{cu}(t) + c(t)$ and $z_d(t) = -z_{cu}(t) + c(t)$, respectively. As seen from the animal's eye, this corresponds to a square at a horizontal distance $y(t) = vt$ from the eye, whose spatial position may be obtained by projecting back its image (Fig. 1A, gray square and dashed lines). If Z_u and Z_d denote the upper and lower edge of the square, respectively, and Z_c its center, then again

by similar triangles, $Z_u(t) = z_u(t)\, y(t)/d_{as}$ and $Z_d(t) = z_d(t)\, y(t)/d_{as}$. Plugging in the expressions for z_u and z_d derived above, we immediately see that $Z_u(t) - Z_d(t) = 2l$ and the center of the object is given by $Z_c = Z_d + l$. Using the above expressions for Z_d, z_d and $y(t)$, we find

$$Z_c(t) = \frac{\alpha v}{d_{as}} t^2 + \frac{z_0 v}{d_{as}} t$$

Thus, the simulated object is approaching the animal with a decelerating vertical velocity, mimicking a swooping approach. The parameters of this vertical component of the approach trajectory are best characterized relative to those of the horizontal approach:

$$\frac{Z_c(t)}{Y(t)} = \frac{t}{\beta} + \gamma,$$

where $\gamma = z_0/d_{as} = 0.61$ and $\beta = d_{as}/\alpha = \pm 6653$ ms.

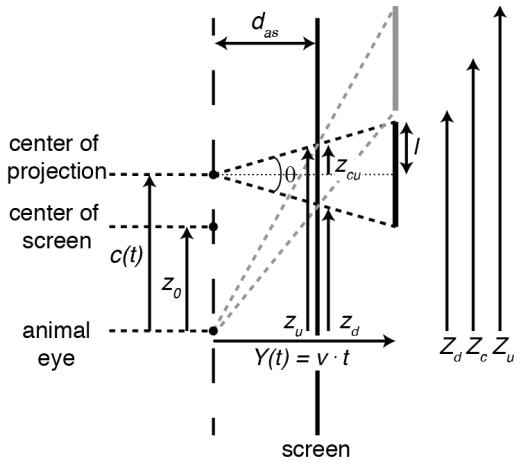

Figure A1. Schematics illustrating how the stimuli were generated and their appearance from the animal's eye.

ACKNOWLEDGEMENTS

Research funding to this project from National Science Foundation (IOS-0904063), the Human Frontier Science Program and the Air Force Research Laboratories is acknowledged.

REFERENCES

[1] Uvarov, B., *Grasshoppers and Locusts, Centre for Overseas Pest Research,* Vol 2, London, 1977.

[2] Baker, P.S., Gewecke, M. and Cooter, R.J., The Natural Flight of the Migratory Locust, *Locusta migratoria* L. III. Wing-Beat Frequency, Flight Speed and Attitude, *J. comp. Physiol.*, A 141, 1981, 233-237.

[3] Ellington, C., Vandenberg, C., Wilmot, A. and Thomas, A., Leading-edge Vortices in Insect Flight, *Nature*, 384, 1996, 626-630.

[4] Dickinson M.H., Lehmann, F.O. and Sane, S.P., Wing Rotation and the Aerodynamic Basis of Insect Flight, *Science,* 284, 1999, 1954-1960.

[5] Walker, G.T., The Flapping Flight of Birds, *J. R. Aero. Soc.*, 29, 1925, 590-594.

[6] Walker, G.T., The Flapping Flight of Birds. II., *J. R. Aero, Soc.*, 31, 1927, 337-342.

[7] Holst, E.V. and Kuchemann, D., Biological and Aerodynamical Problems in Animal Flight, *J. R. Aero. Soc.,* 46, 1942, 39-56.

[8] Osborne, M.F.M, Aerodynamics of Flapping Flight with Application to Insects, *J. Exp. Biol*, 28, 1951, 221-245.

[9] Weis-Fogh, T., Biology and Physics of Locust Flight. II. Flight Performance of the Desert Locust (Schistocerca gregaria), *Phil. Trans. R. Soc. London.,* B239, 667,1956, 459-510.

[10] Weis-Fogh, T. and Jensen, M., Biology and Physics of Locust Flight. I. Basic Principles in Insect Flight - A Critical Review, *Phil. Trans. R. Soc. Lond.,* B239, 1956, 415-458.

[11] Jensen, M., Biology and Physics of Locust Flight. III. The Aerodynamics of Locust Flight, *Phil. Trans. R. Soc. Lond.,* B239, 1956, 511-552.

[12] Cloupeau, M., Devillers, J.F. and Devezeaux, D., Direct Measurements of Instantaneous Lift in Desert Locust; Comparison with Jensen's Experiments on Detached Wings, *J. Exp. Biol.* 80, 1979, 1-15.

[13] Wilkin, P.J., Instantaneous Force on a Desert Locust, *Schistocerca gregaria* (Orthoptera: Acrididae), Flying in a Wind Tunnel. *J. Kansas Entomol. Soc.,* 63, 1990, 316-328.

[14] Dudley, R. and Ellington, C.P., Mechanics of Forward Flight in Bumblebees. II Quasi-Steady Lift and Power Requirements. *J. Exp. Biol.,* 148, 1990, 53-88.

[15] Sane, S.P. and Dickinson, M.H., The Control of Flight Force by a Flapping Wing: Lift and Drag Production. *J. Exp. Biol.,* 204, 2001, 2607-2626.

[16] Combes, S.A. and Daniel, T.L., Into Thin Air: Contributions of Aerodynamic and Inertial-Elastic Forces to Wing Bending in the Hawkmoth *Manduca sexta*, *J. Exp. Biol.,* 206, 2003, 2999-3006.

[17] Mountcastle, A.M. and Daniel, T.L., Aerodynamic and Functional Consequences of Wing Compliance, *Exp. Fluids* 46, 2009, 873-882. (doi:10.1007/s00348-008-0607-0).

[18] Sims, T.W., Palazotto, A.N. and Norris, A., A structural Dynamic Analysis of a Manduca sexta Forewing, *International Journal of Micro Air Vehicles*, 2(3), 2010, 119-140

[19] Walker S.M., Thomas A.L.R. and Taylor, G.K., Photogrammetric Reconstruction of High Resolution Surface Topographies and Deformable Wing kinematics of tethered locusts and free-flying hoverflies., *J. R. Soc. Interface*, 2008, 1-16. (doi:10.1098/rsif.2008.0245).

[20] Walker S.M., Thomas A.L.R. and Taylor, G.K., Deformable Wing Kinematics in the Desert Locust: How and Why do Camber, Twist and Topography Vary through the Stroke, *J. R. Soc. Interface,* 2008, 1-16. (doi:10.1098/rsif.2008.0245).

[21] Taylor, G.K. and Thomas, A.L.R., Dynamic Flight Stability in the Desert Locust *Schistocerca gregaria*, *J. Exp. Biol.,* 206, 2003, 2803-2829.

[22] Taylor, G.K. and Zbikowski, R., Nonlinear Time-Periodic Models of the Longitudinal Flight Dynamics of Desert Locusts *Schistocerca gregaria*, *J. R. Soc. Interface 2*, 2005, 197-221. (doi:10.1098/rsif.2005.0036).

[23] Fotowat, H. and Gabbiani, F., Collision Detection as a Model for Sensory-Motor Integration, *Annu. Rev. Neurosci.*34, 2011, 1-19.

[24] Rind, F. C. and Simmons, P. J., Signaling of Object Approach by the DCMD Neuron of the Locust, *J. Neurophysiol*, 77, 1997, 1029-1033.

[25] Gabbiani, F., Krapp, H.G. and Laurent, G., Computation of object Approach by a Wide-Field, Motion-Sensitive Neuron, *J. Neurosci,* 19, 1999a, 1122-1141.

[26] Judge, S.J. and Rind, F.C., The locust DCMD, a Movement-Detecting neuron Tightly Tuned to Collision Trajectories, *J. Exp. Biol.*, 200, 1997, 2209-2216.

[27] Robertson, R.M. and Reye, D.N., Wing Movements Associated with Collision-Avoidance Maneuvers during flight in the Locust, *Locusta migratoria*, *J. Exp. Biol.*, 163, 1992, 231-258.

[28] Robertson, R.M. and Johnson A.G., Collision Avoidance of Flying Locusts: Steering Torques and Behavior, *J. Exp. Biol.*, 183, 1993, 35-60.

[29] Gray, J.R., Lee, J.K. and Robertson, R.M., Activity of Descending Contralateral Movement Detector Neurons and Collision Avoidance Behavior in Response to Head-on Visual Stimuli in Locusts, *J. comp. Physiol.*, A 187, 2001**,** 115-129.

[30] Santer, R.D., Simmons, P.J. and Rind, F.C., Gliding Behavior Elicited by Lateral Looming Stimuli in Flying Locusts, *J. Comp. Physiol.*, A 191, 2005**,** 61-73.

[31] Rind, F.C., Santer, R.D. and Wright G.A., Arousal Facilitates Collision Avoidance Mediated by a Looming Sensitive Visual Neuron in a Flying Locust, *J Neurophysiol.,* 100, 2008, 670-680.

[32] Chan R.W.M. and Gabbiani, F., Collision avoidance behaviors of minimally restrained flying locusts to looming stimuli, *submitted*.

[33] Figliola, R.S. and Beasley, D.E., *Theory and Design for Mechanical Measurements*, 4th Edition, 2006, John Wiley & Sons Inc.

[34] Baker, P.S. and Cooter, R.J., The Natural Flight of the Migratory Locust, Locusta *migratoria* L. II. Gliding, *J. Comp. Physiol.*, 131, 1979**,** 89-94.